Supporting Information for "Dynamic Bayesian networks for evaluation of Granger causal relationships in climate reanalyses"

Dylan Harries[1]and Terence J. O'Kane[1]

[1]CSIRO Oceans and Atmosphere, Hobart, Australia

Contents of this file

1. Figures S1 to S15
2. Tables S1 to S2

Introduction

This supporting information provides the patterns corresponding to the teleconnection indices analyzed in the main text, summaries of the edge posterior distributions for the alternative choice of hyperparameters, and summaries of the maximum a posteriori (MAP) structure estimates for the fits presented in the main text.

Corresponding author: Dylan Harries, CSIRO Oceans and Atmosphere, Hobart, Australia. (Dylan.Harries@csiro.au)

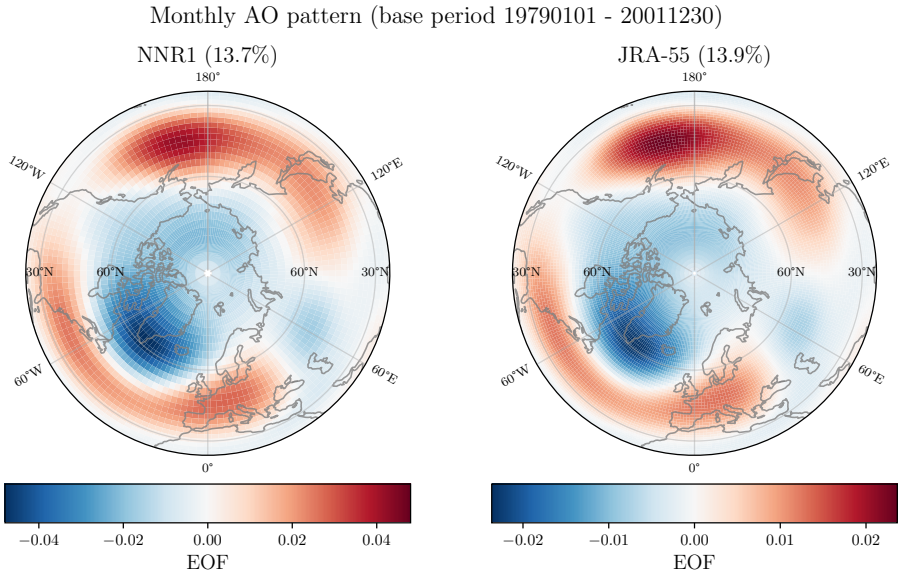

Figure S1. AO loading pattern of 500 hPa geopotential height anomalies in NNR1 (left) and JRA-55 (right).

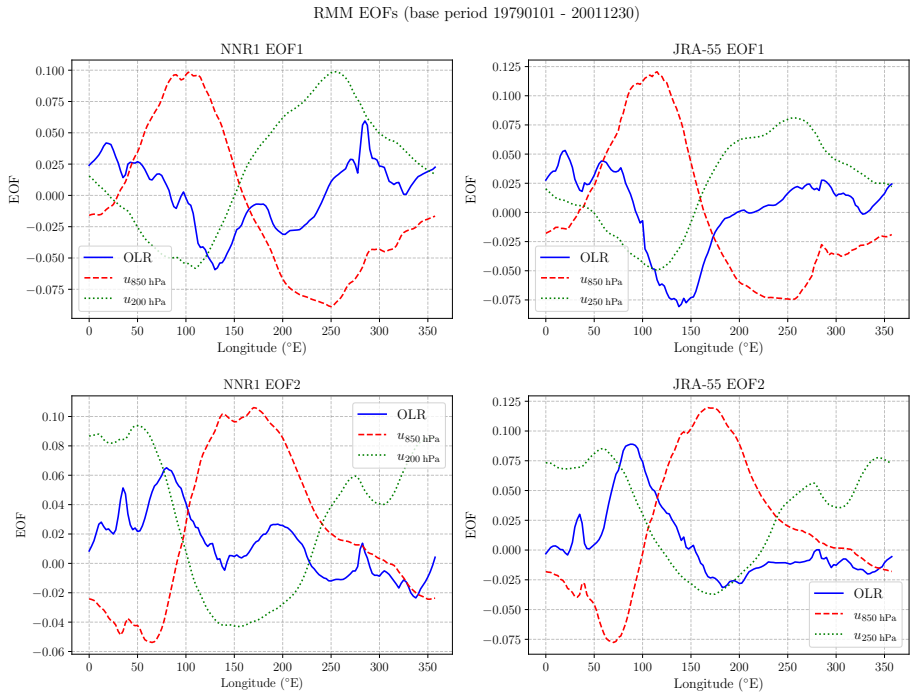

Figure S2. RMM EOFs in HadISST and NNR1 (left column) and JRA-55 (right column).

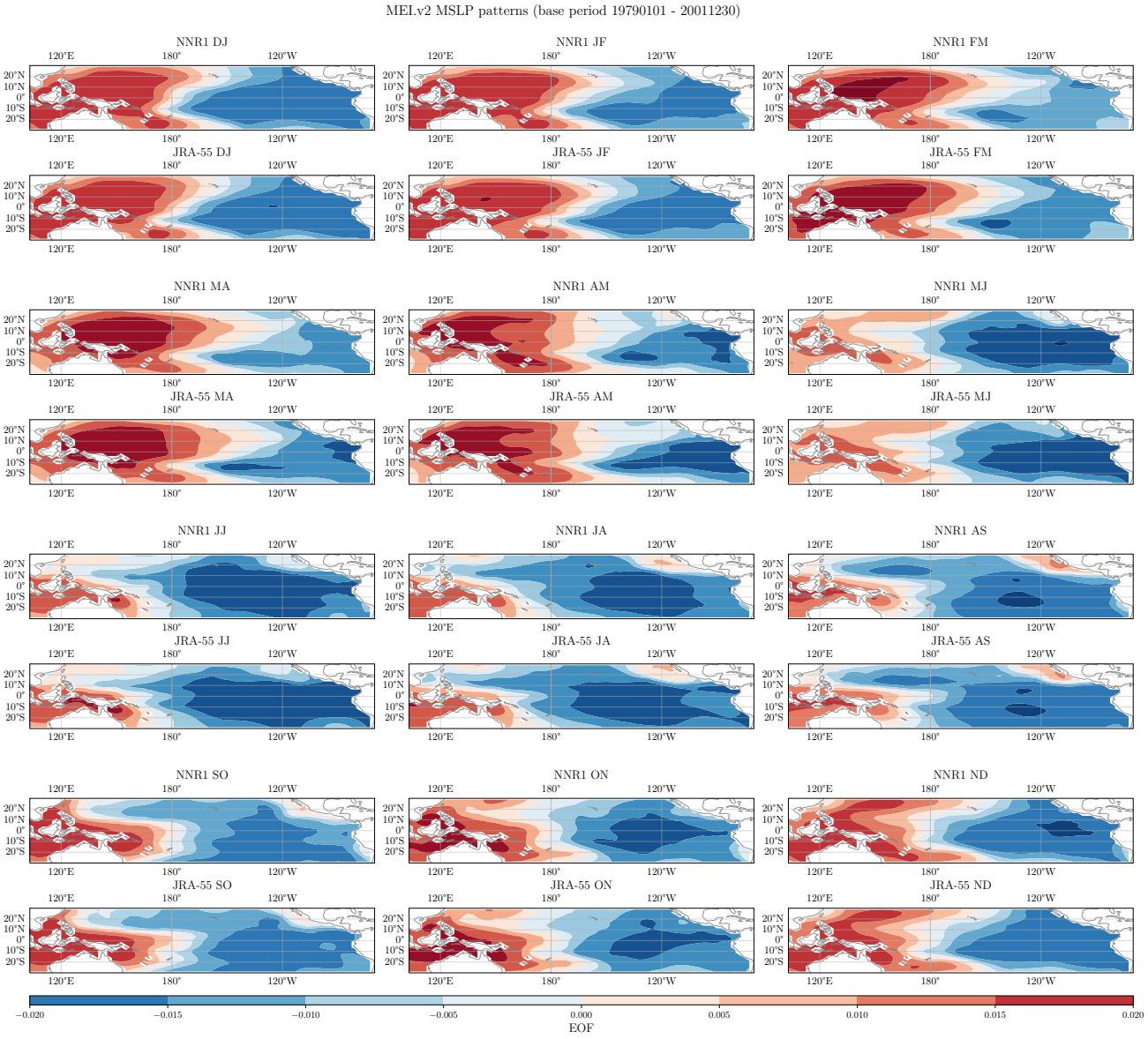

Figure S3. Seasonal MSLP anomaly patterns contributing to the MEI in HadISST and NNR1 (odd numbered rows) and JRA-55 (even numbered rows).

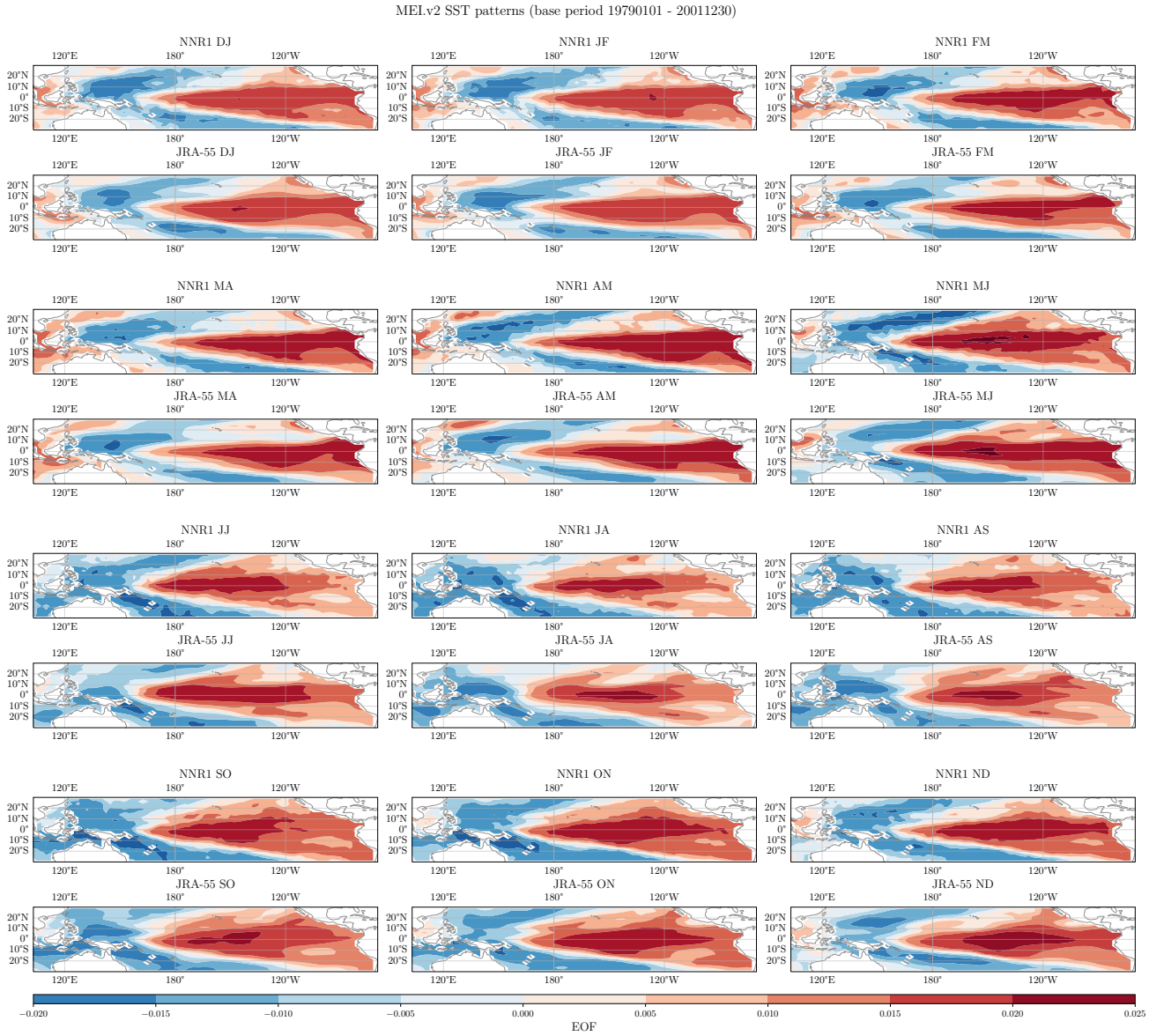

Figure S4. Seasonal SST anomaly patterns contributing to the MEI in HadISST and NNR1 (odd numbered rows) and JRA-55 (even numbered rows).

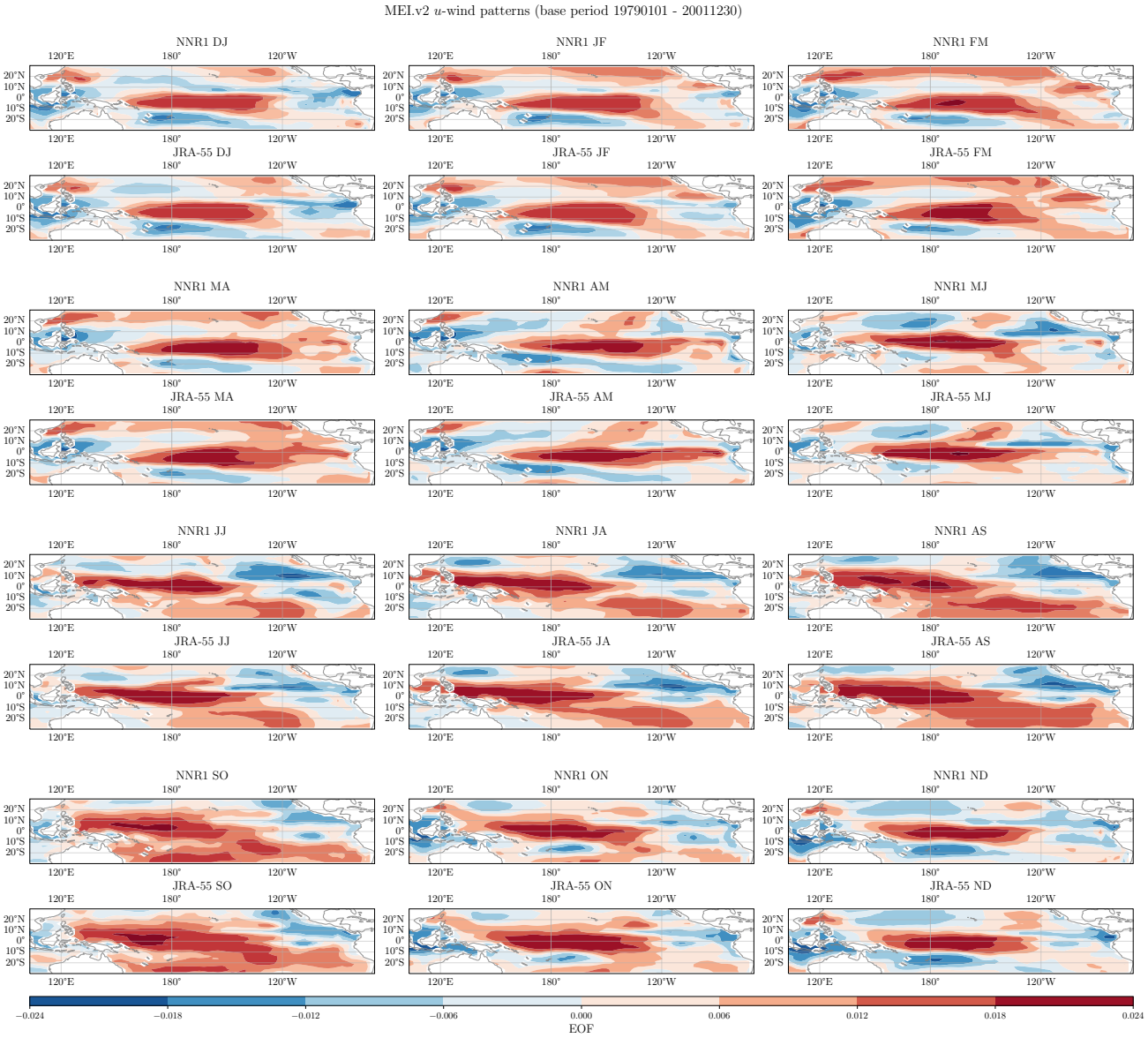

Figure S5. Seasonal zonal wind anomaly patterns contributing to the MEI in HadISST and NNR1 (odd numbered rows) and JRA-55 (even numbered rows).

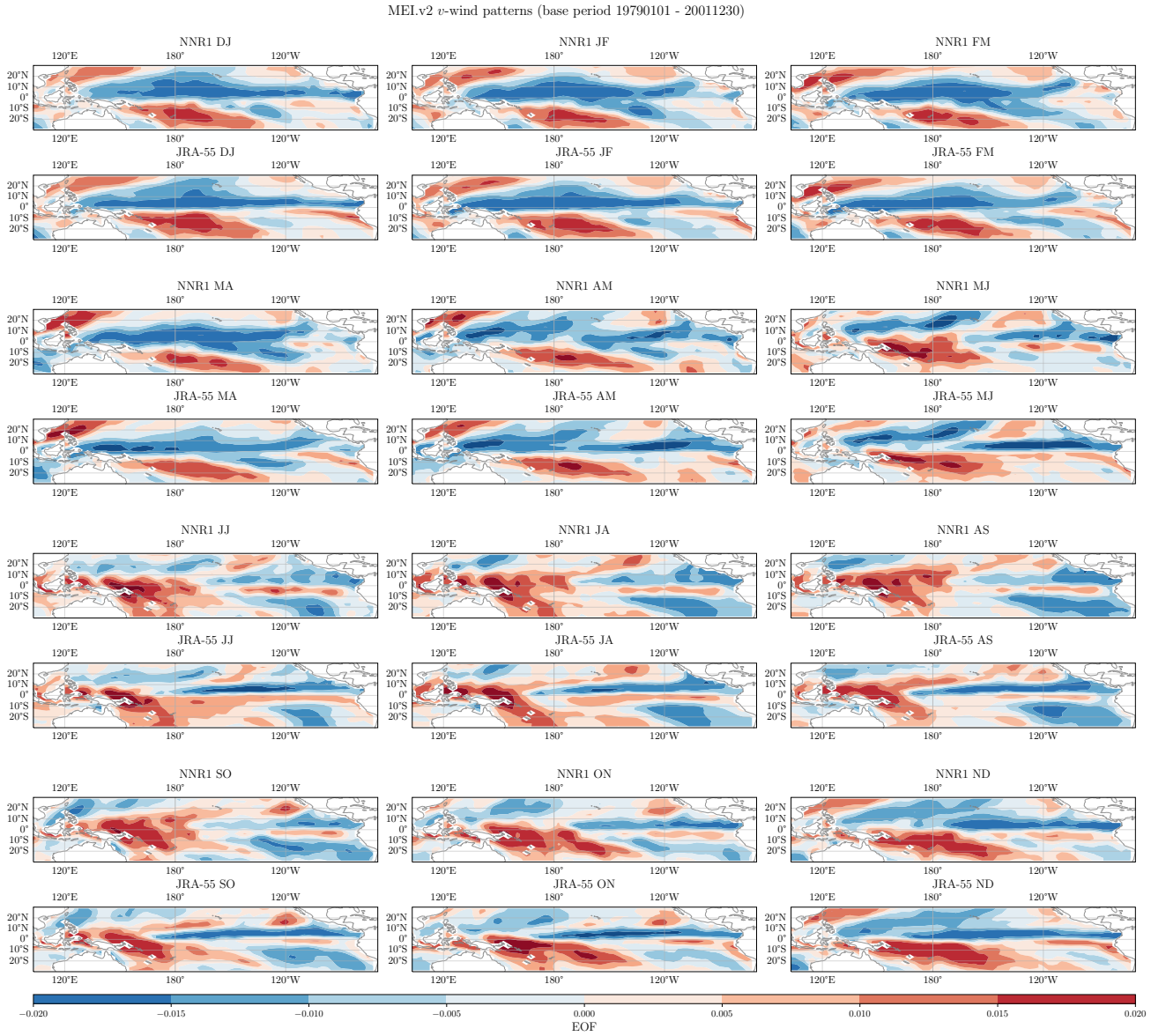

Figure S6. Seasonal meridional wind anomaly patterns contributing to the MEI in HadISST and NNR1 (odd numbered rows) and JRA-55 (even numbered rows).

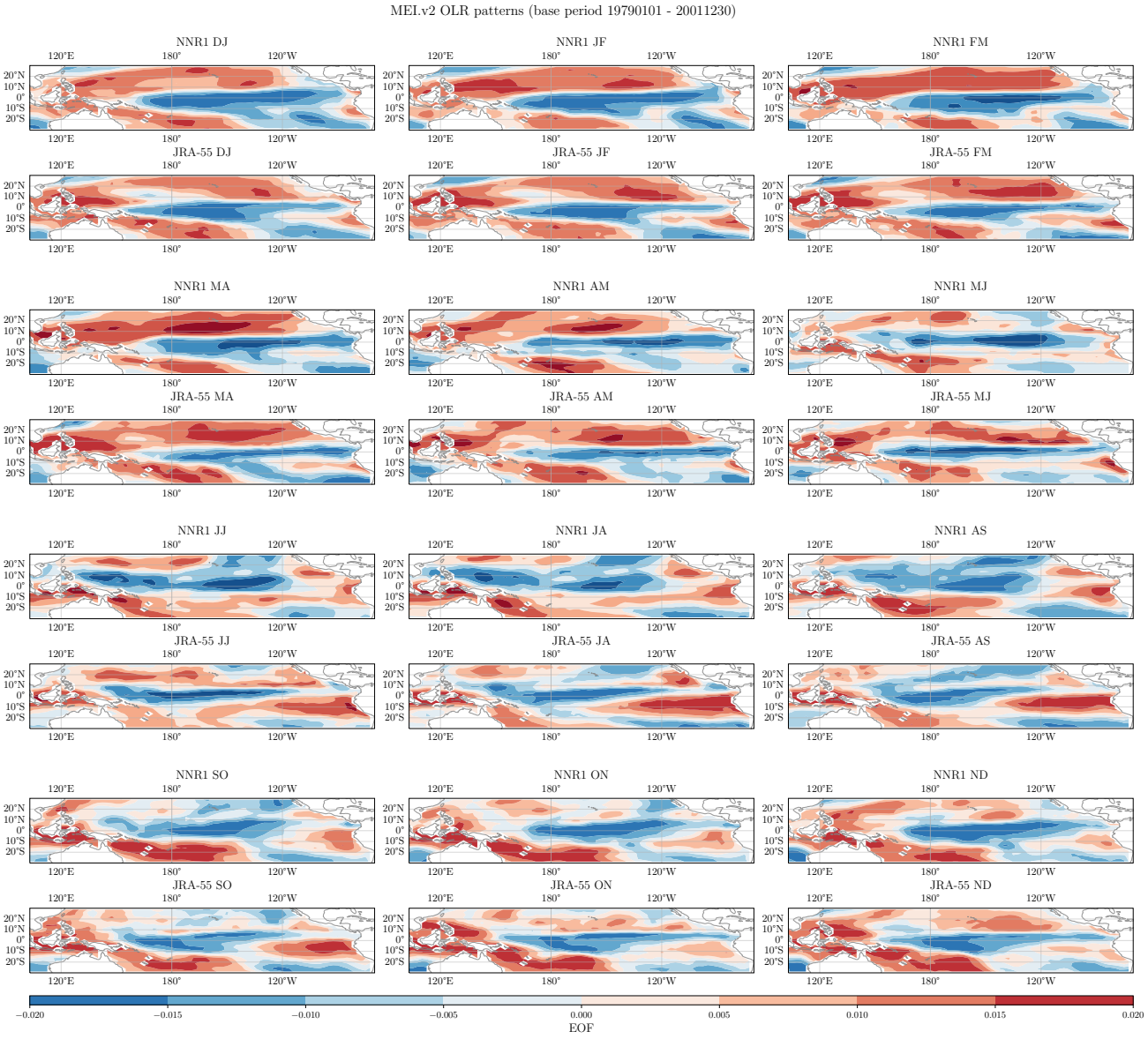

Figure S7. Seasonal OLR anomaly patterns contributing to the MEI in HadISST and NNR1 (odd numbered rows) and JRA-55 (even numbered rows).

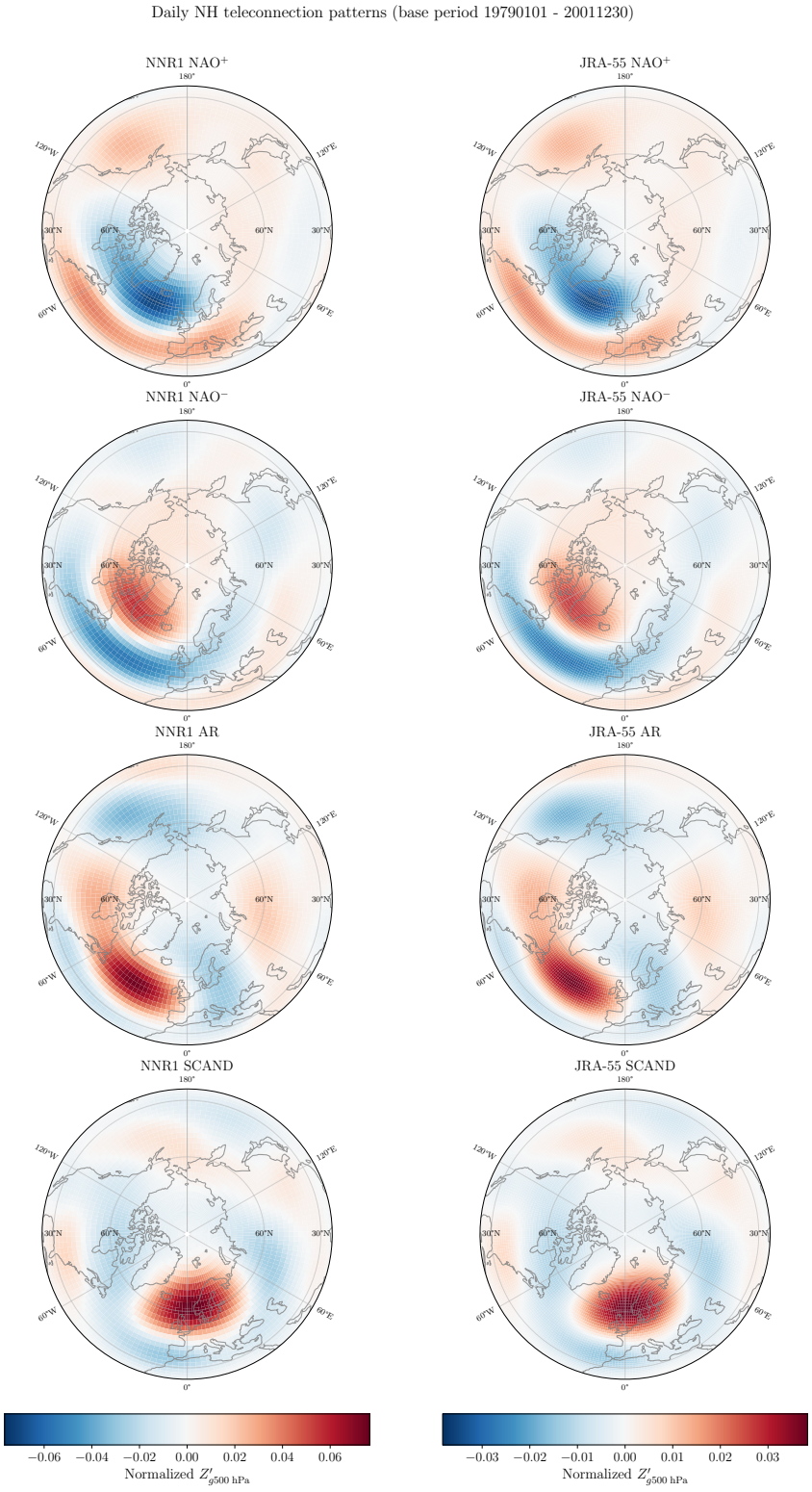

Figure S8. Northern hemisphere cluster loading patterns of 500 hPa geopotential height anomalies in NNR1 (left column) and JRA-55 (right column).

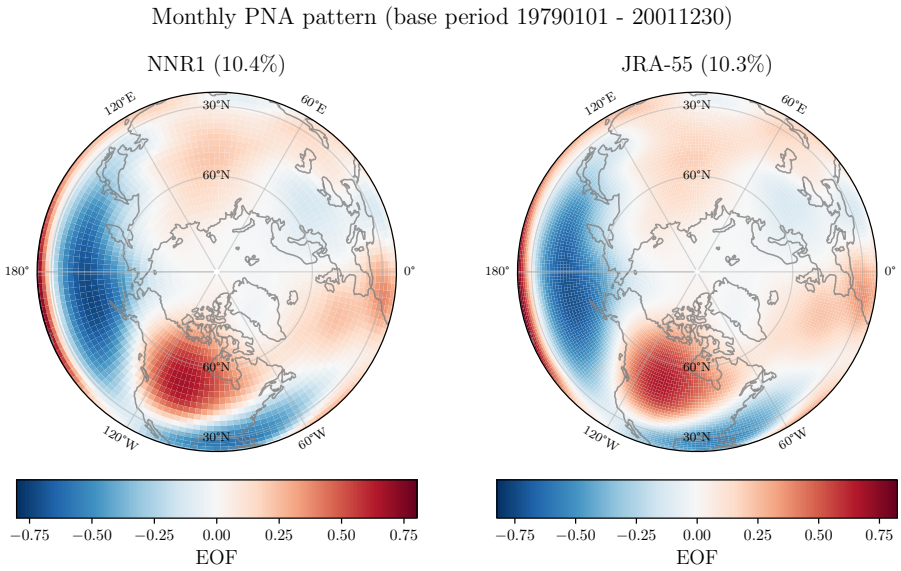

Figure S9. PNA loading pattern of 500 hPa geopotential height anomalies in NNR1 (left) and JRA-55 (right).

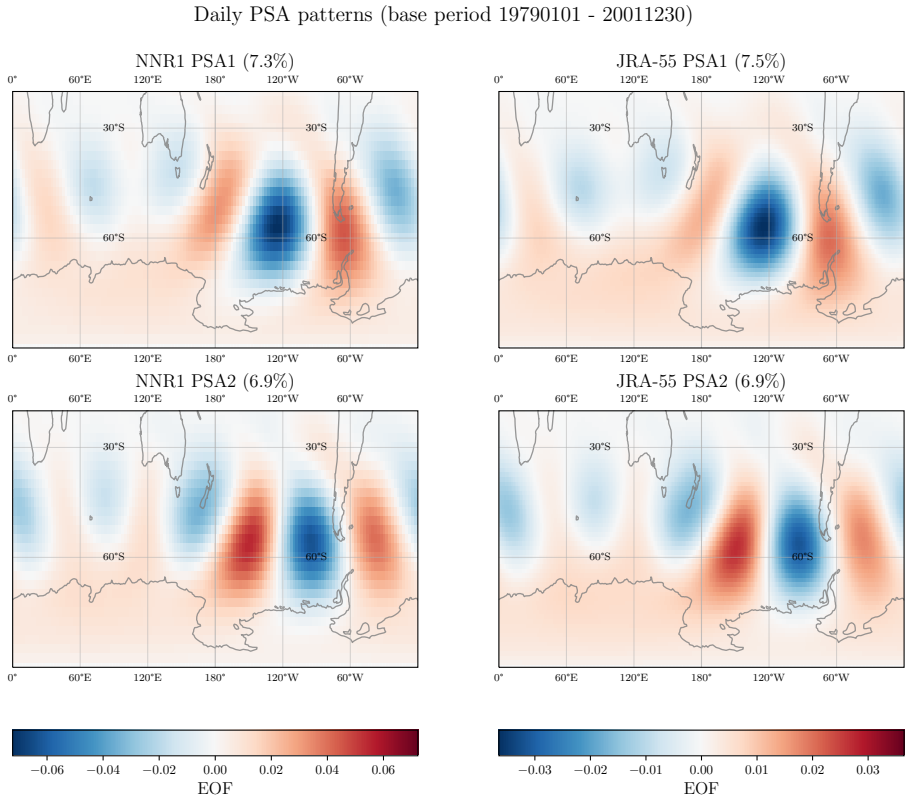

Figure S10. PSA loading patterns of 500 hPa geopotential height anomalies in NNR1 (left) and JRA-55 (right).

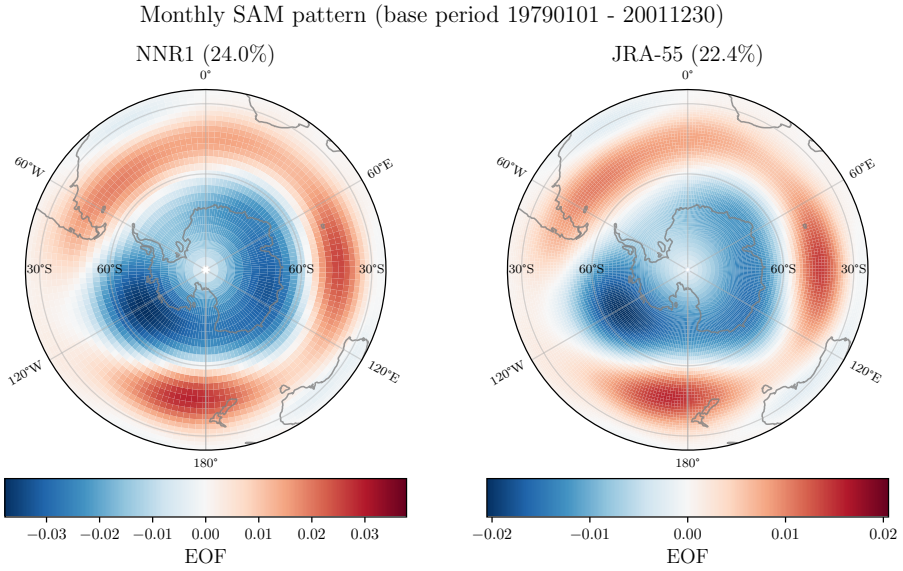

Figure S11. SAM loading pattern of 500 hPa geopotential height anomalies in NNR1 (left) and JRA-55 (right).

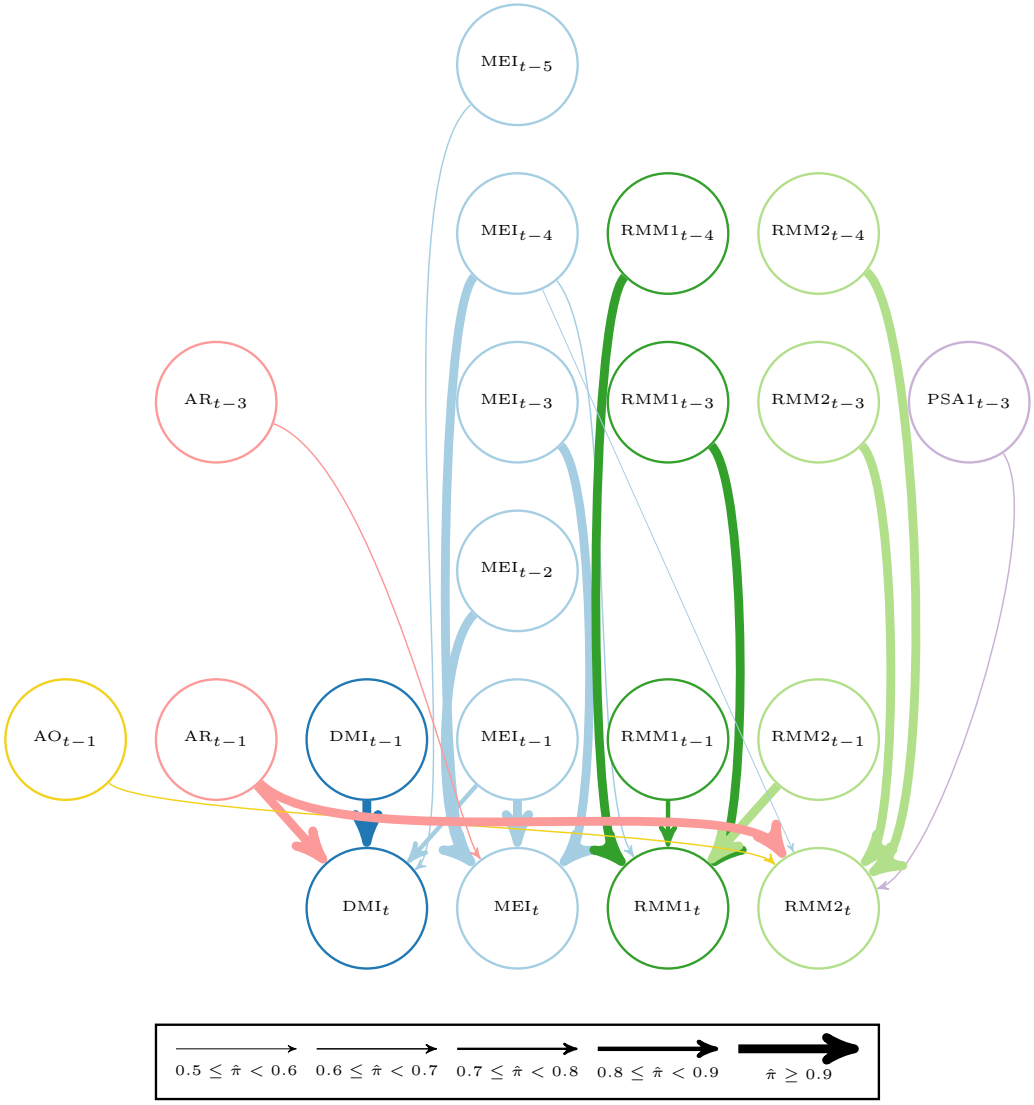

Figure S12. Subgraphs corresponding to the fitted parent sets of the tropical indices in NNR1 based on full-year data for $a_\tau = 0.5$, $b_\tau = 10$, and $\nu^2 \approx 2$. All edges with an estimated posterior probability $\hat{\pi}$ greater than 0.5 are shown.

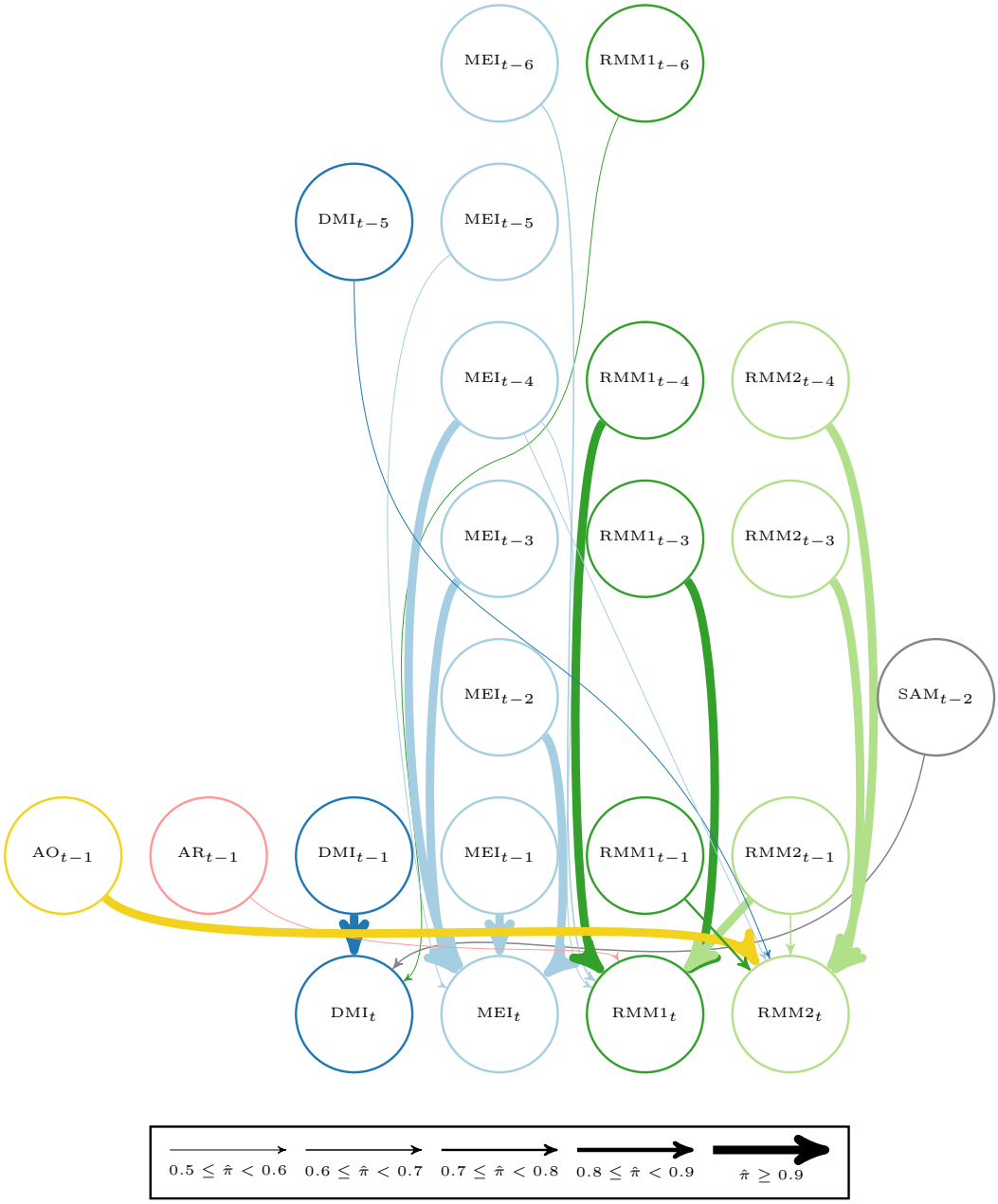

Figure S13. Subgraphs corresponding to the fitted parent sets of the tropical indices in JRA-55 based on full-year data for $a_\tau = 0.5$, $b_\tau = 10$, and $\nu^2 \approx 2$. All edges with an estimated posterior probability $\hat{\pi}$ greater than 0.5 are shown.

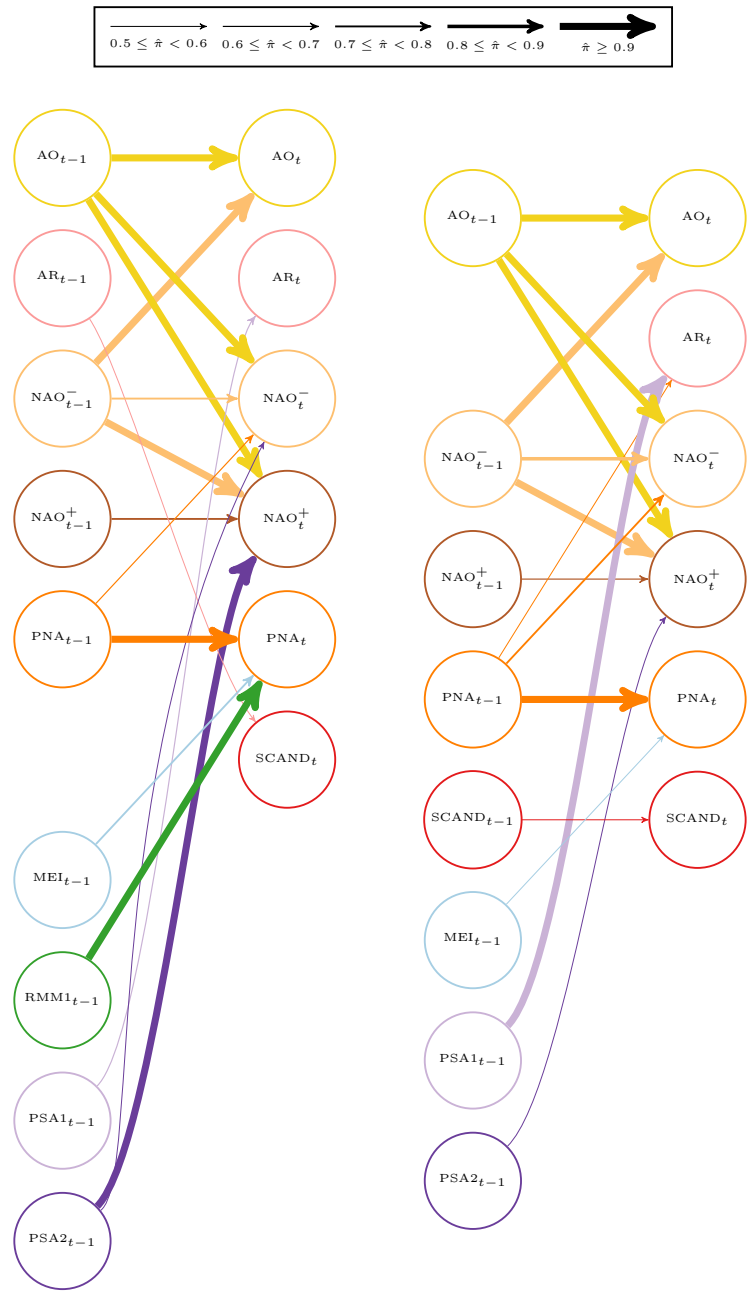

(a) NNR1 NH extratropical, all seasons (b) JRA-55 NH extratropical, all seasons

Figure S14. Subgraphs corresponding to the fitted parent sets of the NH extratropical indices in (a) NNR1 and (b) JRA-55 for $a_\tau = 0.5$, $b_\tau = 10$, and $\nu^2 \approx 2$. All edges with an estimated posterior probability $\hat{\pi}$ greater than 0.5 are shown.

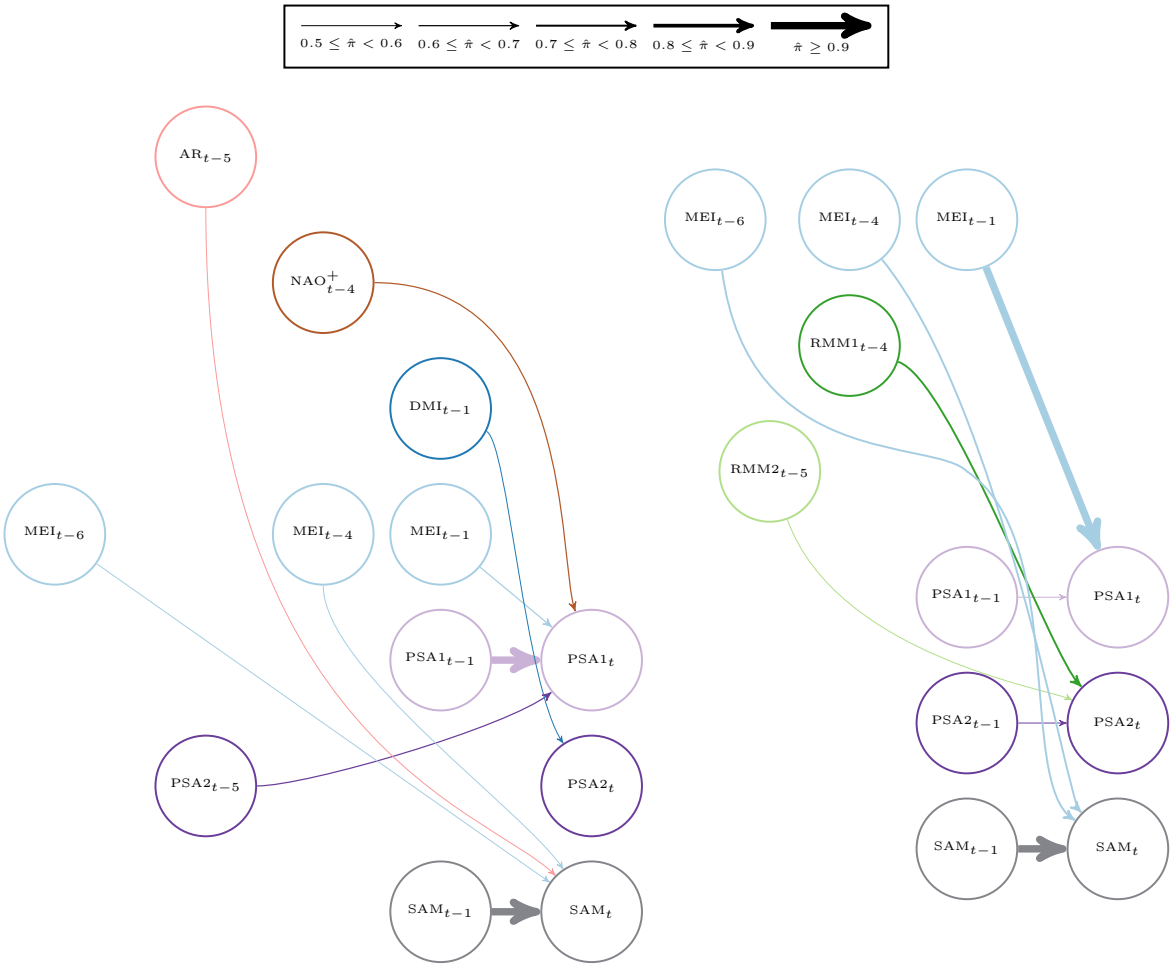

(a) NNR1 SH extratropical, all seasons

(b) JRA-55 SH extratropical, all seasons

Figure S15. Subgraphs corresponding to the fitted parent sets of the SH extratropical indices in (a) NNR1 and (b) JRA-55 for $a_\tau = 0.5$, $b_\tau = 10$, and $\nu^2 \approx 2$. All edges with an estimated posterior probability $\hat{\pi}$ greater than 0.5 are shown.

Table S1. MAP parent sets for monthly tropical teleconnection indices across all seasons for NNR1 and JRA-55 for fits with $a_\tau = 1.5$, $b_\tau = 20$, and $\nu^2 = 3$, showing the estimated posterior probability $\hat{\pi}$ of the edge, the mean parameter value $\hat{\beta}$ conditional on the MAP structure, and the 95% posterior HDI. Dashes indicate a node that is not in the MAP parent set for a given reanalysis.

	JRA-55			NNR1		
Parent node	$\hat{\pi}$	$\hat{\beta}$	95% HDI	$\hat{\pi}$	$\hat{\beta}$	95% HDI
DMI_t						
DMI_{t-1}	1.00	0.63	$(0.56, 0.69)$	1.00	0.74	$(0.68, 0.79)$
SAM_{t-2}	0.59	0.09	$(0.03, 0.16)$	0.33	–	–
MEI_{t-1}	0.22	–	–	0.80	0.13	$(0.06, 0.20)$
MEI_{t-5}	0.08	–	–	0.65	-0.14	$(-0.21, -0.07)$
AR_{t-1}	0.04	–	–	0.94	0.10	$(0.05, 0.16)$
MEI_t						
MEI_{t-1}	1.00	1.45	$(1.37, 1.54)$	1.00	1.43	$(1.34, 1.51)$
MEI_{t-2}	1.00	-0.85	$(-1.00, -0.70)$	1.00	-0.73	$(-0.87, -0.59)$
MEI_{t-3}	1.00	0.65	$(0.49, 0.80)$	1.00	0.38	$(0.24, 0.52)$
MEI_{t-4}	1.00	-0.48	$(-0.63, -0.31)$	0.98	-0.15	$(-0.23, -0.07)$
MEI_{t-5}	0.65	0.28	$(0.13, 0.42)$	0.17	–	–
MEI_{t-6}	0.57	-0.14	$(-0.22, -0.06)$	0.10	–	–
NAO^+_{t-2}	0.38	0.04	$(0.01, 0.06)$	0.17	–	–
AO_{t-2}	0.06	–	–	0.46	0.05	$(0.02, 0.07)$
AR_{t-3}	0.05	–	–	0.66	-0.04	$(-0.07, -0.02)$
$\mathrm{RMM2}_{t-3}$	0.34	–	–	0.41	0.04	$(0.01, 0.06)$
$\mathrm{RMM1}_t$						
MEI_{t-3}	0.47	-0.37	$(-0.49, -0.24)$	0.37	–	–
MEI_{t-6}	0.61	0.24	$(0.13, 0.36)$	0.33	–	–
AR_{t-1}	0.54	-0.12	$(-0.20, -0.04)$	0.24	–	–
$\mathrm{PSA1}_{t-3}$	0.38	-0.14	$(-0.22, -0.05)$	0.11	–	–
SAM_{t-3}	0.34	-0.13	$(-0.20, -0.04)$	0.09	–	–
$\mathrm{RMM1}_{t-1}$	0.40	-0.12	$(-0.19, -0.04)$	0.86	-0.14	$(-0.21, -0.06)$
$\mathrm{RMM1}_{t-3}$	0.99	-0.17	$(-0.25, -0.09)$	0.97	-0.16	$(-0.24, -0.08)$
$\mathrm{RMM1}_{t-4}$	1.00	-0.20	$(-0.27, -0.12)$	1.00	-0.19	$(-0.27, -0.11)$
$\mathrm{RMM2}_{t-1}$	0.99	-0.17	$(-0.25, -0.09)$	1.00	-0.20	$(-0.27, -0.12)$
MEI_{t-4}	0.58	–	–	0.59	-0.45	$(-0.68, -0.22)$
MEI_{t-5}	0.41	–	–	0.35	0.34	$(0.11, 0.57)$
$\mathrm{RMM2}_t$						
AO_{t-1}	0.94	0.18	$(0.10, 0.26)$	0.63	0.15	$(0.07, 0.23)$
DMI_{t-5}	0.50	-0.12	$(-0.20, -0.04)$	0.06	–	–
MEI_{t-4}	0.56	-0.15	$(-0.23, -0.07)$	0.52	–	–
AR_{t-1}	0.44	0.13	$(0.05, 0.21)$	0.93	0.16	$(0.08, 0.24)$
$\mathrm{RMM1}_{t-1}$	0.71	0.13	$(0.05, 0.21)$	0.26	0.14	$(0.06, 0.22)$
$\mathrm{RMM2}_{t-1}$	0.61	-0.13	$(-0.21, -0.05)$	0.45	–	–
$\mathrm{RMM2}_{t-3}$	1.00	-0.24	$(-0.32, -0.16)$	0.98	-0.16	$(-0.23, -0.08)$
$\mathrm{RMM2}_{t-4}$	0.94	-0.17	$(-0.25, -0.09)$	0.94	-0.16	$(-0.24, -0.09)$
MEI_{t-1}	0.10	–	–	0.22	-0.18	$(-0.26, -0.10)$
AR_{t-6}	0.03	–	–	0.33	-0.11	$(-0.19, -0.04)$
$\mathrm{PSA1}_{t-3}$	0.05	–	–	0.59	-0.13	$(-0.22, -0.05)$
$\mathrm{RMM1}_{t-5}$	0.03	–	–	0.20	0.11	$(0.03, 0.19)$
$\mathrm{RMM2}_{t-2}$	0.02	–	–	0.16	0.13	$(0.05, 0.20)$

Table S2. MAP parent sets for monthly SH extratropical teleconnection indices across all seasons for NNR1 and JRA-55 for fits with $a_\tau = 1.5$, $b_\tau = 20$, and $\nu^2 = 3$, showing the estimated posterior probability $\hat{\pi}$ of the edge, the mean parameter value $\hat{\beta}$ conditional on the MAP structure, and the 95% posterior HDI. Dashes indicate a node that is not in the MAP parent set for a given reanalysis.

	JRA-55			NNR1		
Parent node	$\hat{\pi}$	$\hat{\beta}$	95% HDI	$\hat{\pi}$	$\hat{\beta}$	95% HDI
$\mathrm{PSA1}_t$						
MEI_{t-1}	0.94	−0.15	$(-0.23, -0.07)$	0.68	−0.13	$(-0.21, -0.05)$
NAO^+_{t-4}	0.39	−0.11	$(-0.20, -0.04)$	0.60	−0.13	$(-0.21, -0.05)$
$\mathrm{PSA1}_{t-1}$	0.49	0.12	$(0.04, 0.21)$	0.96	0.16	$(0.08, 0.24)$
$\mathrm{PSA2}_{t-5}$	0.17	–	–	0.58	−0.12	$(-0.21, -0.04)$
$\mathrm{PSA2}_t$						
$\mathrm{PSA1}_{t-4}$	0.31	0.12	$(0.03, 0.20)$	0.30	–	–
$\mathrm{PSA2}_{t-1}$	0.49	0.12	$(0.04, 0.21)$	0.34	–	–
$\mathrm{RMM1}_{t-4}$	0.73	0.14	$(0.05, 0.21)$	0.43	–	–
$\mathrm{RMM2}_{t-5}$	0.47	0.12	$(0.04, 0.20)$	0.41	–	–
DMI_{t-1}	0.07	–	–	0.54	−0.14	$(-0.23, -0.06)$
SAM_t						
MEI_{t-4}	0.75	−0.30	$(-0.45, -0.16)$	0.51	–	–
MEI_{t-6}	0.76	0.27	$(0.13, 0.42)$	0.54	–	–
SAM_{t-1}	1.00	0.29	$(0.21, 0.37)$	1.00	0.32	$(0.24, 0.40)$